Eur. Phys. J. B **54**, 291–297 (2006)
DOI: 10.1140/epjb/e2007-00005-y

THE EUROPEAN PHYSICAL JOURNAL B

Interatomic potential effects on dynamical heterogeneities in liquid SiO_2

V.V. Hoang[a]

Dept. of Physics, Institute of Technology, HoChiMinh City National University, 268 Ly Thuong Kiet Str., Distr. 10, HochiMinh City, Vietnam

Received 16 February 2006 / Received in final form 29 November 2006
Published online 13 January 2007 –

Abstract. Dynamical heterogeneities (DH) in low density liquid SiO_2 have been investigated by molecular dynamics (MD) method. Simulations were done in the basic cube under periodic boundary conditions containing 3000 particles with the pair interatomic potentials, which have a weak electrostatic interaction and a Morse type short range interaction (PMSI). We have evaluated the non-Gaussian parameter for the self part of the van Hove correlation function and we found a clear evidence of the existence of DH in low density liquid SiO_2. Moreover, the atomic displacement distribution (ADD) in a model has been obtained and it deviates from a Gaussian form. The results have been compared with those obtained in another liquid SiO_2 system with the Born-Mayer interatomic potentials (BMP) in order to observe the interatomic potential effects on the DH in the system and indeed, the effects are strong. Calculations showed that particles of extremely low or fast mobility have a tendency to form a cluster and mean cluster size of most mobile and immobile particles in PMSI models increases with decreasing temperature. In contrast, no systematic changes have been obtained for the most mobile and immobile particles in BMP models. Calculations show that there is no relation between local particle environment and particle mobility in the system.

PACS. 61.43.Fs Glasses – 78.55.Qr Amorphous materials; glasses and other disordered solids – 61.43.Bn Structural modeling: serial-addition models, computer simulation – 61.20.Lc Time-dependent properties; relaxation

1 Introduction

DH in the simulated supercooled oxides has attracted great interest in recent years. Kerrache et al. investigated the presence of DH in MD simulated supercooled silica with BKS interatomic potentials by comparing the partial radial distribution functions (PRDFs) for the 10% most mobile particles with the corresponding mean ones at the temperatures of 3500 K and 5000 K [1]. No DH was found at high temperature of 5000 K and the DH appeared during the cooling procedure when the temperature decreased. Moreover, the O and Si particles showed similar heterogeneities but with different rate of change during aging [1]. Somewhat later, spatially heterogeneous and dynamic facilitation in a larger model of viscous silica containing 8016 particles with the BKS interatomic potentials have been observed [2]. Calculations showed that high particle mobility predominantly propagated continuously through the melt supported the concept of dynamic facilitation [2]. Furthermore, temperature dependence of spatially heterogeneous dynamics in this model of viscous silica above and below the critical temperature of the mode-coupling theory has been found [3]. It was found that on the intermediate time scales small fraction of particles was more mobile than expected from a Gaussian approximation and they formed clusters. Calculations showed that mean cluster size is maximum at times intermediate between ballistic and diffusive motion and the maximum size increases with decreasing temperature, and moreover, the growth of clusters continues when the diffusion constants follow an Arrhenius law [3]. The DH in supercooled Al_2O_3 have been observed in a model containing 3000 particles with the Born-Mayer interatomic potentials [4,5] via the calculations of the non-Gaussian parameter and PRDFs of 5% (or 10%) most mobile or immobile particles in the system. It was found that the most mobile or immobile particles in supercooled Al_2O_3 were strongly correlated and they formed clusters. It was found there is no relation between particle mobility and local environments of the particles [5] unlike those observed previously in Lennard-Jones liquids [6]. Furthermore, we found a clear evidence of cooling rate effects on the DH in supercooled Al_2O_3 and these effects are quite different for the most mobile and immobile particles in the system [7]. And recently, DH in simulated liquid GeO_2 has been found [8].

[a] e-mail: vvhoang2002@yahoo.com

Concerning on the vitreous SiO_2, while the system at high density of around 2.20–2.30 g/cm^3 has been under intensive investigations for past three decades, it was spent less attention to the low density one. It is well-known that the porosity strongly affects on the structure and properties of the vitreous systems [9]. So far, the feature of DH in liquids is still not well understanding and the interatomic potential effects on DH in liquids have not been investigated yet. Therefore, it motivates us to carry out the detailed investigations of the interatomic potential effects on DH in vitreous silica at low density of 1.83 g/cm^3. It is essential to notice that for the first time the interatomic potential effects on DH in the silica system have been studied.

2 Calculations

We performed MD simulations of supercooled silica in a 3000-particle system (1000 Si particles and 2000 O particles) under periodic boundary conditions. We have carried out two independent studies, in the first study we use the interatomic potentials which are of the form:

$$U_{ij}(r) = \frac{q_i q_j}{r} + D_0 \left\{ \exp\left[\gamma\left(1 - \frac{r}{R_0}\right)\right] - 2\exp\left[\frac{1}{2}\gamma\left(1 - \frac{r}{R_0}\right)\right]\right\} \quad (1)$$

where q_i and q_j represent the charges of atoms i and j, for Si atom $q_{\mathrm{Si}} = +1.30e$ and for O atom $q_{\mathrm{O}} = -0.65e$ (e is the elementary charge unit); r denotes the interatomic distance between ith and jth atoms; D_0, γ and R_0 are the parameters of the Morse potentials represented the short-range interaction in the system. The Morse potential parameters for silica system can be found in references [10,11] as given below.

In the second study, we use the Born-Mayer interatomic potentials which have the form:

$$U_{ij}(r) = \frac{q_i q_j}{r} + B_{ij}\exp\left(-\frac{r}{R_0}\right) \quad (2)$$

where $q_{\mathrm{Si}} = +4.0e$ and $q_{\mathrm{O}} = -2.0e$; $B_{\mathrm{SiSi}} = 0$ eV; $B_{\mathrm{SiO}} = 1729.5$ eV; $B_{\mathrm{OO}} = 1500$ eV and $R_0 = 29$ pm. These interatomic potentials described well both structure and atomization energy of liquid and amorphous silica and details about these potentials can be found in [12,13].

Simulations were done at constant volume corresponding to the low density of vitreous silica of 1.83 g/cm^3. We use the Verlet algorithm with the MD time step of 1.6 fs, Coulomb interactions were taken into account by the Ewald-Hansen method [12,13]. The initial equilibrium state at the temperature of 7000 K has been obtained by the equilibrating a random configuration model of 3000 particles for over 40 000 MD time steps or 64 ps. In order to simulate the cooling process, we take this configuration as the starting point of a constant volume run in which the temperature of the system was decreased linearly in time as $T(t) = T_0 - \gamma t$, where γ is the cooling rate of 4.2945×10^{13} K/s and T_0 is the initial temperature of 7000 K. This cooling process is continued until the temperature of the system is equal to 350 K. The so-obtained configurations at finite temperatures were subsequently relaxed for 80 ps before investigation of static and dynamic properties. In order to improve the statistics, the results have been averaged over two independent runs. In order to calculate the coordination number distributions and bond-angle distributions in liquid and amorphous SiO_2, we adopt the fixed values $R_{\text{Si-Si}} = 3.30$ Å, $R_{\text{Si-O}} = 2.10$ Å and $R_{\text{O-O}} = 3.00$ Å. Here R denotes a cut-off radius, which is chosen as the position of the minimum after the first peak in the PRDFs for the silica system at 2100 K.

Table 1. Parameters of the Morse type part of the potentials.

Interaction	D_0 (eV)	γ	R_0 (Å)
Si-Si	0.0077	15.3744	3.7598
Si-O	1.9960	8.6342	1.6280
O-O	0.0233	10.4112	3.7910

3 Results and discussions

Before discussing about DH in the system, we turn our attention to some structural properties of liquid silica at low density. Figure 1 and Table 2 show that structure of models obtained by using BMP and PMSI at the same temperature of 2100 K slightly differs from each other and it has a slightly distorted tetrahedral network with the mean coordination number $Z_{\text{Si-O}} \approx 4.0$ and $Z_{\text{O-Si}} \approx 2.0$. The simulated results are close to the experimental data for vitreous silica. More details about the local structure can be inferred from the coordination number and bond-angle distributions in the system (Figs. 2 and 3). However, in this work we study only the most important distributions such as distributions of O-Si-O and Si-O-Si angles (Fig. 3). The first one describes the order inside structural units and the second one describes the connectivity between them. For an ideal tetrahedral network structure, the O-Si-O angle is of 109.47°, and for our model at 2100 K such angle is equal to 105.2° or 106.2° for models obtained by using BMP and PMSI, respectively. Meanwhile, the calculated mean Si-O-Si angle is equal to 160.5° and 152.3°, respectively for the same models and it is larger than that observed in experiment for the amorphous silica, which is equal to 147° (see Refs. [15,16]). It is true that our models are looser than those sample used in experiments due to low density used in simulation here (i.e. it is equal to 1.83 g/cm^3 versus the value around 2.20 g/cm^3 at the ambient conditions in practice). Figure 2 shows that coordination number distributions for the Si-Si and O-O pairs of models obtained by using BMP and PMSI at the same density of 1.83 g/cm^3 are different from each other, while it is similar for other pairs. In contrast, Si-O-Si bond-angle distributions are quite different from each other contrary to the O-Si-O angle distributions (Fig. 3).

Table 2. Structural characteristics of liquid and amorphous SiO_2. r_{ij} — Positions of the first peaks in the partial radial distribution functions (PRDFs) $g_{ij}(r)$; Z_{ij} — The average coordination number.

References	r_{ij} (Å)			Z_{ij}				$\theta_{\text{O-Si-O}}$	$\theta_{\text{Si-O-Si}}$
	Si-Si	Si-O	O-O	Si-Si	Si-O	O-Si	O-O		
Data of present work at 2100 (K)[a]	3.09	1.51	2.50	4.00	4.00	2.00	6.07	105.2°	160.5°
Data of present work at 2100 (K)[b]	3.08	1.54	2.57	3.87	3.95	1.97	6.14	106.2°	152.3°
Calculated data at 2000 (K) in [12][c]	3.17	1.62	2.59		4.00	2.00		109.1°	152.7°
Calculated data at 1923 K in [14][d]	3.17	1.64	2.65	5.13	4.39		7.28		
Experimental data at 300 K in [15,16]	3.12	1.62	2.65		4.00	2.00		109.5°	147°

[a] The data obtained by using BMP at the density of 1.83 g/cm^3; [b] the data obtained by using PMSI at the density of 1.83 g/cm^3; [c] the data obtained by using BMP at the density of 2.20 g/cm^3; [d] the data obtained by using the BELION algorithm at the density of 2.20 g/cm^3.

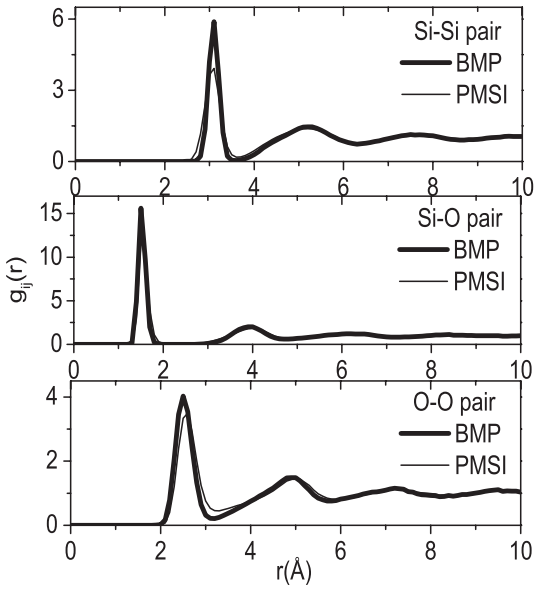

Fig. 1. Partial radial distribution functions in SiO_2 models obtained at 2100 K by using two different interatomic potentials.

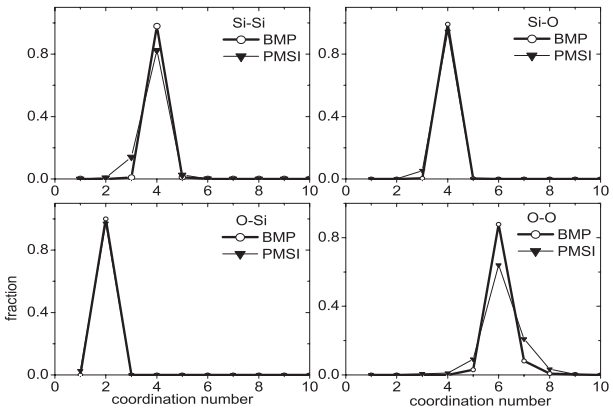

Fig. 2. Coordination number distributions in SiO_2 models obtained at 2100 K by using two different interatomic potentials.

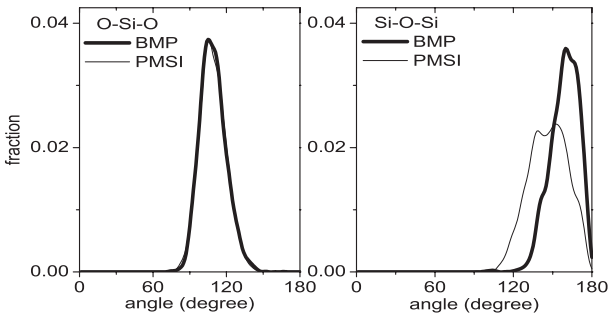

Fig. 3. Bond-angle distributions in SiO_2 models obtained at 2100 K by using two different interatomic potentials.

This implies that models are different mainly by the connectivity between structural units SiO_x rather than by the order inside them. Moreover, we can see in Table 2 that structure of silica model at low density of 1.83 g/cm^3 not much differs from those obtained at higher density of 2.20 g/cm^3. On the other hand, significant differences in PRDFs, coordination number and bond-angle distributions might strongly affect the dynamics of two models which will be investigated in detail in next section.

Further, we would like to present the effects of interatomic potentials on other two important quantities of the system such as glass transition temperature, T_g, and mean-squared atomic displacement, $\langle r^2(t)\rangle$, of atomic species. The evolution of potential energy of the silica models obtained by using two interatomic potentials upon cooling from the melt is represented in Figure 4. The glass transition temperature can be determined via the intersection of a linear high- and low-temperature extrapolation of the potential energy which is equal to $T_g \approx 2376$ K for BMP model and to $T_g \approx 2080$ K for PMSI one. Such value for T_g is higher than that observed in practice for silica which is equal to $T_g \approx 1450$ K [17]. The discrepancy may be related to the different density used in simulation and in experiment. Moreover, due to time scale restriction and small size of the system used in simulation deviation of simulated value for T_g from the experimental one can be expected. On the other hand, $T_g \approx 2080$ K for PMSI model is also higher than the value $T_g = 1400$ K obtained by the analysis of bonding information of models obtained by using the same interatomic potentials with higher density [11]. Finally, results obtained here show a clear effect

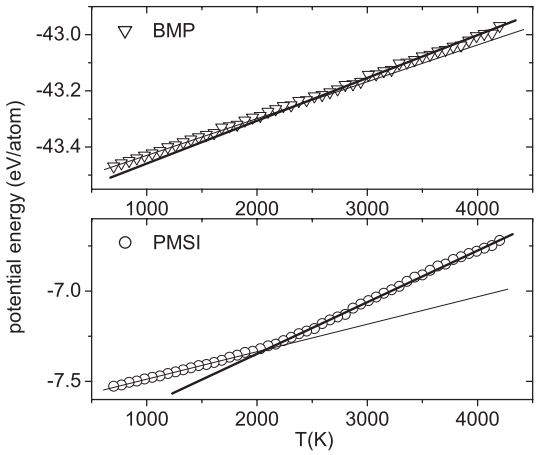

Fig. 4. Temperature dependence of potential energy of SiO_2 models obtained by using two different interatomic potentials.

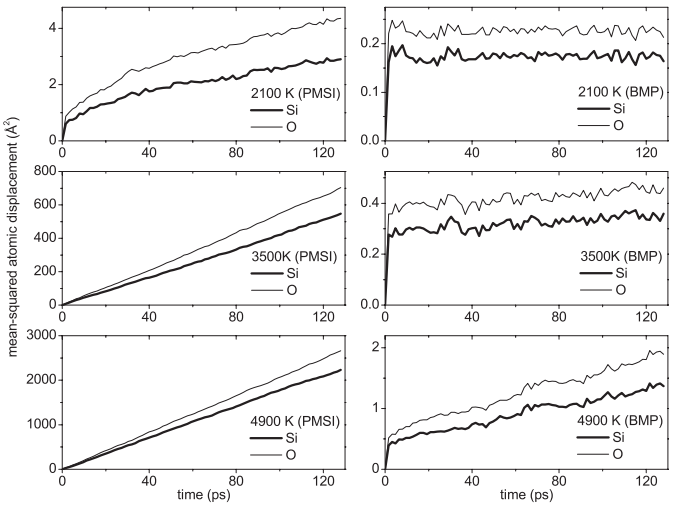

Fig. 5. Time dependence of mean-squared atomic displacement, $\langle r^2(t)\rangle$, of atomic species in SiO_2 models obtained by using two different interatomic potentials.

of interatomic potentials on T_g of the system and it is in good accordance with those previously obtained for silica, i.e. one finds $T_g \approx 2000$ K with the Tsuneyuki potential [18] and $T_g \approx 2900$ K with the BKS potential [19]. The effects of interatomic potentials on the mean-squared atomic displacement, $\langle r^2(t)\rangle$, of atomic species in SiO_2 models have been found which is different from each other in several orders of magnitude at the same temperatures (Fig. 5). It was found that the dynamics of the system are much sensitive on the potentials used in simulation rather than the static properties and it may lead to different diffusion constants of atomic species [20]. The time dependence of $\langle r^2(t)\rangle$ has two common regimes: the ballistic one at the beginning short time and the diffusive one at longer time (Fig. 5). Due to very low dynamics in model with BMP, there is a clear onset of glasslike dynamics at around 2100 K whereas it occurs at lower temperature for model with PMSI. And it is in good accordance with

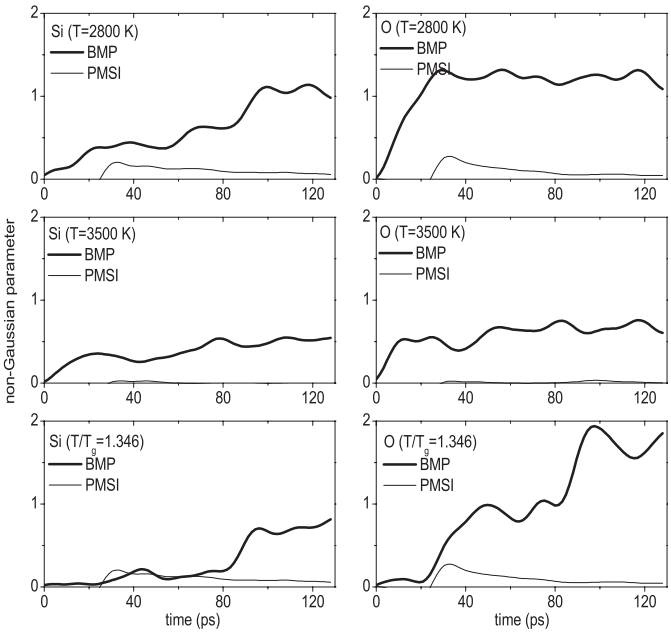

Fig. 6. Non-Gaussian parameter $\alpha_2(t)$ in liquid SiO_2 models obtained at three different temperatures by using two different interatomic potentials.

those observed for glass transition temperature T_g of two systems (see Fig. 4).

3.1 Non-Gaussian parameter and atomic displacement distribution

And now, we stop here for the discussion about the DH in the system which can be detected via the calculating non-Gaussian parameter $\alpha_2(t) = \frac{3\langle r^4(t)\rangle}{5\langle r^2(t)\rangle^2} - 1$, or directly through the atomic displacement distributions (ADD). For a dynamically homogeneous system $\alpha_2(t) \approx 0$, as shown in Figure 6 this parameter in liquid SiO_2 models obtained at three different temperatures differs from zero indicating the existence of DH in the liquid silica which has a tendency to enhance with decreasing temperature. In order to improve the statistics, the results have been averaged over two independent runs. Figure 6 shows that $\alpha_2(t)$ in silica systems obtained by using two different potentials is quite different from each other in terms of the position and heights of peaks in the curves. It seems that small peaks in the curves for PMSI model are related to not good statistics of our results (i.e. averaging only over two independent runs). However, the situation for the curves of BMP model is quite different because there are several large peaks. At all temperatures investigated (i.e. 3500 K, 2800 K and $T/T_g \approx 1.346$), DH in BMP model is stronger than those in PMSI one. This means that we found a clear evidence of interatomic potential effects on the DH in the system.

On the other hand, in a homogeneous liquid ADD has a Gaussian form and deviations from this form also show the existence of DH in the system. According to our calculations for the 80 ps relaxed liquid silica models ADD

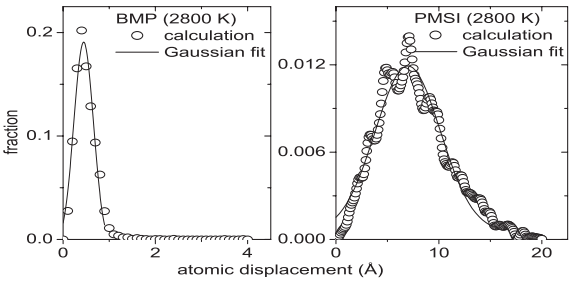

Fig. 7. Atomic displacement distributions in liquid SiO_2 models obtained at 2800 K by using two different interatomic potentials.

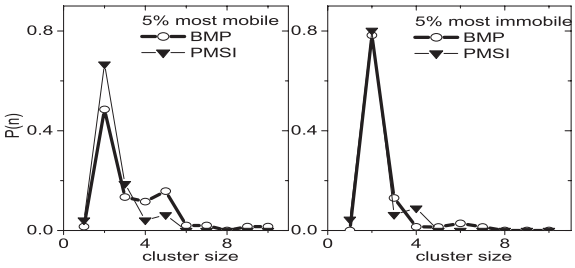

Fig. 8. The probability distribution $P(n)$ of clusters of size n for 5% most mobile and immobile particles in liquid SiO_2 models obtained at 2800 K by using two different interatomic potentials.

deviates from a Gaussian form by a tail of more mobile particles. We can infer approximately from these ADDs fraction of the most mobile particles in the system, and for PMSI model it is equal to 3.0% (we account both Si and O particles together in a tail of the curve, i.e. particles have an atomic displacement larger than 15.00 Å after relaxation time of 80 ps, see Fig. 7). In contrast, it is about 5.60% in BMP model (i.e. both Si and O particles together with an atomic displacement larger than 0.90 Å after relaxation time of 80 ps, see Fig. 7). These values are not very far from 5% in Lennard-Jones liquids [21] and in charged colloidal suspensions [22] or 6.5% in glass-forming polymer melt [23]. The discrepancy between the data of two models in present work indicates again the interatomic effects on DH in the system. On the other hand, the fraction of most mobile particles in the system also depends on the temperature [24]. However, for convenience we will use the fixed value of 5% as often taken in many other works to identify the most mobile or immobile particles in our liquid silica.

3.2 Spatial correlations

It was found that particles of extremely low or fast mobility have a tendency to form a cluster upon cooling and we detect this problem in our liquid silica via an investigation of cluster size distributions of the 5% most mobile or immobile particles in liquid SiO_2 models obtained at 2800 K. For determination of cluster of particles we have used the same rule as was done in references [4,5,21], that is, two particles belong to the same cluster if their distance is less than the radius of the nearest neighbor shell. The radii of the nearest-neighbor shells are defined by the first minimum in PRDFs, $g_{ij}(r)$, and we have adopted the fixed values $R_{\text{Si-Si}} = 3.30$ Å, $R_{\text{Si-O}} = 2.10$ Å and $R_{\text{O-O}} = 3.00$ Å, which were used for calculating the coordination number distributions.

The probability distribution $P(n)$ of clusters of size n in models obtained at 2800 K (Fig. 8) clearly shows that particles of extremely low or fast mobility have a tendency to form clusters and they do not randomly distribute throughout the system. For the 5% most mobile particles, we found one largest cluster containing 24 particles in BMP model or 7 particles in PMSI model. In contrast, for the 5% most immobile particles this number is of 5 particles in both BMP and PMSI models. These numbers are small compared with those observed in other silica models [3]. The discrepancy might be related to the very high silica density used in reference [3] (i.e. equal to 2.37 g/cm^3), and the density dependence of DH in the system will be studied in our subsequent work in this direction. For our case, it seems that the most immobile particles are less correlated than the most mobile ones. It is essential to notice that the probability distribution $P(n)$ presented in Figure 8 differs from those observed for Lennard-Jones liquids [21], charged colloidal suspensions [22]. Possibly, it is caused by the different choices of an interval time Δt for calculating cluster size distribution. Commonly, Δt is chosen as the time when the non-Gaussian parameter $\alpha_2(t)$ or the mean cluster size is maximum and corresponding cluster size distribution shows a power law, $P(n) \sim n^{-\gamma}$ (see Refs. [21,22]). The interval time Δt in current work was adopted to be equal to 80 ps corresponding to a good equilibrated liquid model. One can infer from Figure 5 that the calculations were done in the diffusive regime for both models with different interatomic potentials over whole temperature range studied (i.e. it ranges from 2450 K to 6300 K). It is necessary to carry out the calculations of cluster size distribution in the models obtained at the time when the non-Gaussian parameter $\alpha_2(t)$ or the mean cluster size is maximum like those done in other works. As presented Figure 4 however, the maxima of the non-Gaussian parameter $\alpha_2(t)$ in models obtained by two different interatomic potentials are located very far from each other and such approach is not appropriate for our case.

Temperature dependence of mean cluster size for the 5% most mobile and immobile particles in liquid silica has been found and presented in Figure 9. While mean cluster size of the 5% most mobile and immobile particles in PMSI models increases with decreasing temperature like those often observed in Lennard-Jones liquids [21], silica [3] or in liquid alumina [4], no systematic changes was found for the most mobile and immobile ones in BMP models. After intensive testing we found that temperature dependence of mean cluster size of the most mobile particles in PMSI models is described approximately by an exponential decay law, $S = S_0 + A\exp(-T/t_1)$ with $S_0 = 2.069$, $A = 537.709$ and $t_1 = 370.242$. In Lennard-Jones liquids, temperature dependence of mean cluster size, S, of the

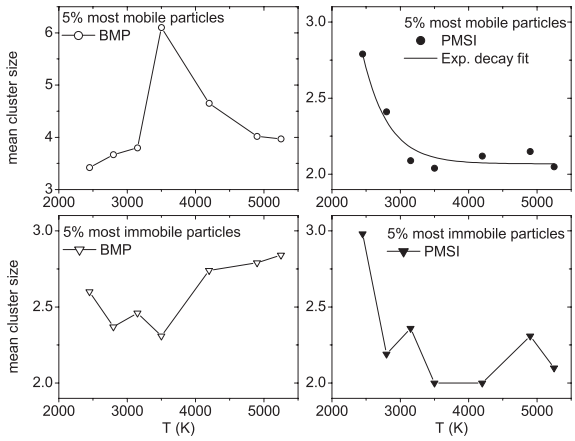

Fig. 9. Temperature dependence of mean cluster sizes for 5% most mobile and immobile particles in liquid SiO_2 models obtained by using two different interatomic potentials after relaxation time of 80 ps.

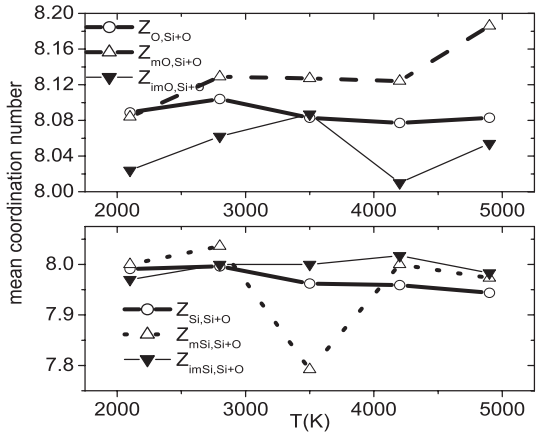

Fig. 10. Mean coordination number of 5% most mobile and immobile particles in liquid SiO_2 at different temperatures compared with those of the mean ones; $Z_{\mathrm{Si,Si+O}}$ and $Z_{\mathrm{O,Si+O}}$ are the average total number of neighbors (both Si and O particles together) of the mean Si and O particles in the model, respectively; $Z_{m\mathrm{Si,Si+O}}$ and $Z_{m\mathrm{O,Si+O}}$ are the average total number of neighbors (both Si and O particles together) of the most mobile Si and O particles in the model, respectively; Analogously for the most immobile Si and O ones we denote $Z_{im\mathrm{Si,Si+O}}$ and $Z_{im\mathrm{O,Si+O}}$.

most mobile particles shows a power law, $S \sim (T - T_p)^{\gamma}$, and in contrast, the mean cluster size of the most immobile particles is relatively constant with T (see Ref. [21]). On the other hand, mean cluster size of the most mobile particles in BKS silica liquids did not show a power law with temperature and it was suggested that the feature of DH in simple liquids can not be generalized to the case of network-former BKS silica [3]. The most immobile particles in BKS silica have not been studied yet [3].

3.3 Surrounding

It was clearly found in Lennard-Jones systems that immobile particles have more neighbors and most mobile particles have fewer neighbors than the average ones [6]. This means that there is a relation between local structure and dynamics in Lennard-Jones system. So far, the features of the DH of supercooled liquids are not well understood and we try to get some insights into the reason for the particle mobility and we also look for possible differences in the local surrounding of 5% most mobile/immobile particles in comparison to average particles in the silica systems obtained by using the Born-Mayer potentials. According to our results (Fig. 10) the phenomenon, observed previously in Lennard-Jones liquid that most mobile particles have less neighbors and most immobile particles have more neighbors than the mean ones, has not been found for our liquid SiO_2. This means that no systematic relation between the local coordination and particle mobility in the BMP SiO_2 system has been found. It is confirming again that the feature of DH in simple liquid can not be generalized for network-forming systems like that stated in reference [3]. Similar results have been obtained for PMSI models (not shown).

4 Conclusions

For the first time the interatomic potential effects on the DH in low density liquid silica have been studied. Our investigations present the existence of DH in liquid silica models obtained by using two different interatomic potentials. However, the feature of DH in both models is quite different and it indicates the interatomic potentials effects on DH in the system as follows:

(i) The non-Gaussian parameters in models obtained at 2800 K, 3500 K and at $T/T_g \approx 1.346$ by using two different interatomic potentials are quite different in terms of the type, the positions and the heights of the peaks of the curves.
(ii) It was found that mean cluster size of the most mobile particles in PMSI models increases with decreasing temperature and it shows an exponential grow law with reduction of temperature while no systematic changes have been found for those in BMP models.
(iii) The spatial correlations of the most mobile or immobile particles for different species in the PMSI and BMP models are quite different.

Similarly, the interatomic potential effects on DH in other systems can be expected. Because the DH in the system can have an important role in the liquid-glass transition, results of our simulations give some ideas for further investigations of DH in supercooled liquids to gain deeper understanding of such phase transition. Different features of DH in the same supercooled liquid might lead to different glass states of the system. Moreover, direct observation of the existence of DH in colloidal systems has been found experimentally [24] and effects of interatomic potentials on the DH in the system can be found experimentally in materials where the interparticle potential can be accurately controlled. For example, in a solution of globular proteins the interaction range can be controlled by changing the ionic strength [25] or in sterically stabilized colloids, the

attraction range can be tuned by changing the grafted chain-chain interaction [26]. And indeed, in a mixture of colloidal particles and a non-adsorbing polymer the length of the polymer fixes the interaction range and the amount of non-adsorbing polymer in solution fixes the interaction strength [27,28].

References

1. A. Kerrache, V. Teboul, D. Guichaoua, A. Monteil, J. Non-Cryst. Solids **322**, 41 (2003)
2. M. Vogel, S.C. Glotzer, Phys. Rev. Lett. **92**, 255901 (2004)
3. M. Vogel, S.C. Glotzer, Phys. Rev. E **70**, 061504 (2004)
4. V.V. Hoang, S.K. Oh, J. Phys.: Condens. Matt. **17**, 5179 (2005)
5. V.V. Hoang, Phys. Stat. Sol. A **203**, 478 (2006)
6. K. Vollmayr-Lee, W. Kob, K. Binder, A. Zippelius, J. Chem. Phys. **116**, 5158 (2002)
7. V.V. Hoang, S.K. Oh, Int. J. Mod. Phys. B **20**, 947 (2006)
8. V.V. Hoang, in *Progress in Solid State Chemistry Research*, edited by R.W. Buckley (Nova Science Publishers, New York, 2006)
9. J. Gross, G. Reichenauer, J. Fricke, J. Phys. D: Appl. Phys. **21**, 1447 (1988)
10. N.T. Huff, E. Demiralp, T. Cagin, W.A. Goddard III, J. Non-Cryst. Solids **253**, 133 (1999)
11. A. Takada, P. Richet, C.R.A. Catlow, G.D. Price, J. Non-Cryst. Solids **345, 346**, 224 (2004)
12. D.K. Belashchenko, Russ. Chem. Rev. **66**, 733 (1997)
13. V.V. Hoang, D.K. Belashchenko, V.T.M. Thuan, Physica B **348**, 249 (2004)
14. D.K. Belashchenko, O.I. Ostrovski, Inorganic Materials **40**, 241 (2004)
15. L.I. Tatarinova, *The structure of solid amorphous and liquid substances* (Nauka Moscow, 1983)
16. R.L. Mozzi, B.E. Warren, J. Appl. Cryst. **2**, 164 (1969); R.L. Mozzi, B.E. Warren, J. Appl. Cryst. **3**, 251 (1970)
17. R. Bruckner, J. Non-Cryst. Solids **5**, 123 (1970)
18. B. Guillot, Y. Guissani, J. Chem. Phys. **104**, 7633 (1996)
19. K. Vollmayr, W. Kob, K. Binder, Phys. Rev. B **54**, 15808 (1996)
20. M. Hemmati, C.A. Angell, in: *Physics Meets Geology*, edited by H. Aoki, R. Hemley (Cambrige University Press, Cambrige, England, 1998)
21. C. Donati, S.C. Glotzer, P.H. Poole, W. Kob, S.J. Plimpton, Phys. Rev. E **60**, 3107 (1999)
22. B.V.R. Tata, P.S. Mohanty, M.C. Valsakumar, Phys. Rev. Lett. **88**, 018302 (2002)
23. Y. Gebremichael, T.B. Schroder, F.W. Starr, S.C. Glotzer, Phys. Rev. E **64**, 051503 (2001)
24. W.K. Kegel, A. van Blaaderen, Science **287**, 290 (2000)
25. F. Sciortino, Nature Mater. **1**, 145 (2002)
26. W.B. Russel, D.A. Saville, W.R. Schowalter, *Colloidal Dispersions* (Cambridge Univ. Press, NewYork, 1989)
27. T. Eckert, E. Barsh, Phys. Rev. Lett. **89**, 125701 (2002)
28. K.N. Pham, A.M. Puertas, J. Bergenholtz, S.U. Egelhaaf, A. Moussaid, P.N. Pusey, A.B. Schofield, M.E. Cates, M. Fuchs, W.C.K. Poon, Science **296**, 104 (2002)